Title

Plasma metabolic profile delineates roles for neurodegeneration, pro-inflammatory damage and mitochondrial dysfunction in the FMR1 premutation.

Journal

Biochemical Journal, 473(21)

ISSN

0264-6021

Authors

Giulivi, Cecilia
Napoli, Eleonora
Tassone, Flora
et al.

Publication Date

2016-11-01

DOI

10.1042/bcj20160585

Peer reviewed

Biochemical Journal (2016) **473** 3871–3888
DOI: 10.1042/BCJ20160585

PORTLAND PRESS

Research Article

Plasma metabolic profile delineates roles for neurodegeneration, pro-inflammatory damage and mitochondrial dysfunction in the *FMR1* premutation

Cecilia Giulivi[1,2], Eleonora Napoli[1], Flora Tassone[2,3], Julian Halmai[1] and Randi Hagerman[2,4]

[1]Department of Molecular Biosciences, School of Veterinary Medicine, University of California Davis, 1089 Veterinary Medicine Dr., VetMed 3B #3009, Davis, CA 95616, USA; [2]Medical Investigation of Neurodevelopmental Disorders (MIND) Institute, University of California Davis, Davis, CA 95817, USA; [3]Department of Biochemistry and Molecular Medicine, School of Medicine, University of California Davis, Davis, CA, USA; and [4]Department of Pediatrics, University of California Davis Medical Center, Sacramento, CA 95817, USA

Correspondence: Cecilia Giulivi (cgiulivi@ucdavis.edu)

Carriers of premutation CGG expansions in the fragile X mental retardation 1 (*FMR1*) gene are at higher risk of developing a late-onset neurodegenerative disorder named Fragile X-associated tremor ataxia syndrome (FXTAS). Given that mitochondrial dysfunction has been identified in fibroblasts, PBMC and brain samples from carriers as well as in animal models of the premutation and that mitochondria are at the center of intermediary metabolism, the aim of the present study was to provide a complete view of the metabolic pattern by uncovering plasma metabolic perturbations in premutation carriers. To this end, metabolic profiles were evaluated in plasma from 23 premutation individuals and 16 age- and sex-matched controls. Among the affected pathways, mitochondrial dysfunction was associated with a Warburg-like shift with increases in lactate levels and altered Krebs' intermediates, neurotransmitters, markers of neurodegeneration and increases in oxidative stress-mediated damage to biomolecules. The number of CGG repeats correlated with a subset of plasma metabolites, which are implicated not only in mitochondrial disorders but also in other neurological diseases, such as Parkinson's, Alzheimer's and Huntington's diseases. For the first time, the identified pathways shed light on disease mechanisms contributing to morbidity of the premutation, with the potential of assessing metabolites in longitudinal studies as indicators of morbidity or disease progression, especially at the early preclinical stages.

Introduction

A modestly expanded CGG nucleotide repeat (55–200) in the 5′-UTR of the fragile X mental retardation gene 1 (*FMR1* [1–3]) represents the genetic hallmark of premutation carriers. Originally, premutation carriers were thought to be free of phenotypic traits; however, reports regarding fragile X-associated primary ovarian insufficiency (FXPOI; [4]), followed by the discovery of fragile X-associated tremor ataxia syndrome (FXTAS; OMIM: 300623), identified in adult carriers [5] discredited this notion. Premutation carriers may also suffer from psychological problems, visuospatial deficits and immune dysregulation [2,3,6–8], and affected children are often diagnosed with ADHD, autism, anxiety and other psychopathologies [9,10]. At the cellular level, fibroblasts from premutation carriers (humans or animal models of the premutation) are generally accompanied by high *FMR1* gene expression, normal or lower levels of fragile X mental retardation protein (FMRP) and mitochondrial dysfunction [11–14].

Currently, premutation carriers include 1 million women and 320 000 men in the USA [15]. It is currently unknown which carriers of the premutation will develop FXTAS. Clinical diagnosis fails to identify those carriers before significant neurological symptoms are evident; thus, there is an

Received: 16 June 2016
Revised: 11 August 2016
Accepted: 23 August 2016

Accepted Manuscript online: 23 August 2016
Version of Record published: 27 October 2016

Biochemical Journal (2016) 473 3871–3888
DOI: 10.1042/BCJ20160585

immediate need for early detection and effective drugs for the cure or the prevention of FXTAS development. An understanding of the molecular characteristics underlying the disease processes of the premutation is a prerequisite for providing therapeutic strategies.

To fulfill this immediate need, metabolic profiling performed on readily accessible body fluids, such as cerebrospinal fluid, serum, urine or saliva, is one of the most important techniques that provide a complete view of the metabolic status and uncovering metabolic perturbations in pathways [16–18] for the diagnosis of many diseases [19], including metabolic disorders [20], motor neuron disease [21], Parkinson's [22] and Alzheimer's diseases [23] as well as chemical toxicity and aging [24–27]. To this end, plasma metabolomics was evaluated in premutation carriers and age- and sex-matched controls, with the aim of providing a complete view of the status of intermediary metabolism with the potential of uncovering perturbations in metabolic pathways [17,18] associated with the presence of the *FMR1* premutation.

Materials and methods

Characteristics of the subjects enrolled in the present study

The study was conducted at the MIND Institute and approved by the IRB ethics committee at UC Davis Medical Center. Exclusion criteria were refusal of the patient or his guardian, infection or malignancy. Blood samples were obtained by venipuncture with informed consent. Controls and carriers of the premutation were recruited through the Fragile X Treatment and Research Center at the MIND Institute at the University of California, Davis, and who participated in our genotype–phenotype study of families with fragile X between the years 2013 and 2015. All blood draws were performed at the MIND Institute between 8 and 10 am (fasting was not advised). No exercise prior to the blood draw was reported; however, it seems an unlikely event since the subjects are usually at the clinic between 7 and 8 am on the day of the examination. Clinical evaluations with Dr Hagerman and associates were performed after the blood draw. CGG repeat number in all individuals included in the present study was evaluated using Southern blot and PCR analysis as described previously [28]. Participants were not excluded from the present study if they were taking prescription medications. However, careful record of all prescription medications was obtained.

Subjects

The 'control group' consisted of 16 individuals (female-to-male ratio = 1.3; mean age ± SD of 37 ± 13 years). The 'premutation group' was constituted by 23 premutation carriers (female-to-male ratio = 1.1; mean age ± SD of 37 ± 19 years; Table 1). Four of the subjects in the premutation group were diagnosed with FXTAS utilizing the criteria by Jacquemont et al. [29]. Of the subjects included in the present study, 6 controls and 13 carriers were on multivitamins/probiotics or nutritional supplements, 1 control and 8 carriers were on antidepressants, 3 controls and 4 carriers on cyclooxygenase inhibitors, 2 controls and 2 carriers on hormone replacement therapy, 1 control and 2 carriers on antihistamines, as well as 1 control and 1 carrier on nitric oxide-producing drugs. Other medications included hydroxymethylglutaryl CoA reductase inhibitors (2 carriers), proton pump inhibitors (2 carriers), β2 agonists (2 carriers), levodopa (1 carrier), α2A receptor agonist (1 carrier), α1 adrenergic blocker (1 control), ACE inhibitor (1 carrier), anticoagulant (1 control), barbiturate (1 carrier), β-blocker (1 carrier) and inhibitor of monoamine transport (1 carrier). Although not significant, carriers were more likely to take vitamins and supplements than controls (56.5 vs. 37.5%; $P = 0.059$).

Sample preparation for metabolomics

The protocol for plasma metabolomics was reported in detail recently [30]. Plasma samples were extracted following the protocols published [31]. Samples were derivatized by methoxyamine hydrochloride in pyridine and subsequently by *N*-methyl-*N*-trimethylsilyltrifluoroacetamide for trimethylsilylation of acidic protons. Data were acquired according to ref. [32]. Absolute spectra intensities were further processed by a filtering algorithm implemented in the metabolomics BinBase database. The BinBase algorithm used the settings: validity of chromatogram (<10 peaks with intensity >107 counts s^{-1}), unbiased retention index marker detection (MS similarity >800, validity of intensity range for high *m*/*z* marker ions) and retention index calculation by fifth-order polynomial regression. Spectra were cut to 5% base peak abundance and matched to database entries from most to least abundant spectra using the following matching filters: retention index window ± 2000 units (equivalent to approximately ±2 s retention time), validation of unique ions and apex masses (unique ion must be included in apexing masses and present at >3% of base peak abundance), mass spectrum similarity must fit

Biochemical Journal (2016) **473** 3871–3888
DOI: 10.1042/BCJ20160585

Table 1. Demographics and clinical characteristics of plasma donors included in the present study.

C and P refer to controls and carriers of the premutation, respectively. The number following the letter identifies the subject from which the plasma samples were obtained

Clinical groups	Age* (years)	CGG repeat expansion†	Sex‡	FXTAS stage
C1	29.0	30	M	0
C2	54.0	30	M	0
C3	23.0	29, 30	F	0
C4	50.5	21	M	0
C5	24.0	30	M	0
C6	41.2	43	M	0
C7	28.8	20, 33	F	0
C8	26.0	30	M	0
C9	33.7	23, 30	F	0
C10	54.0	25, 33	F	0
C11	25.0	24, 33	F	0
C12	45.0	22, 33	F	0
C13	24.0	23, 35	F	0
C14	26.3	30, 37	F	0
C15	41.5	20	M	0
C16	57.4	23, 30	F	0
P1	46.3	61	M	0
P2	9.7	31, 63	F	0
P3	8.4	180	M	0
P4	24.0	31, 93	F	0
P5	19.7	177	M	0
P6	55.6	104	M	0
P7	49.3	31, 86	F	0
P8	17.3	16, 67	F	0
P9	45.3	69	M	0
P10	49.9	20, 98	F	0
P11	9.1	160	M	0
P12	55.4	30, 69	F	0
P13	53.0	16, 67	F	0
P14	33.1	30, 137	F	0
P15	43.2	30, 106	F	0
P16	38.4	33, 60	F	0
P17	8.4	180	M	0
P18	24.0	30, 79	F	0
P19	25.0	67	M	0
P20	62.5	105	M	4
P21	61.3	96	M	4
P22	61.8	110–130	M	1
P23	59.1	33, 107	F	3

*Mean age ± SD = 37 ± 13 years and 37 ± 19 years, respectively, for controls and premutation ($P = 1.000$).
†Mean CGG expansion ± SD = 31 ± 5 and 103 ± 40, respectively, for controls and carriers ($P \leq 0.0001$).
‡Female-to-male ratio = 1.3 and 1.1, respectively, for the control and premutation groups (χ^2 $P = 0.802$).

Biochemical Journal (2016) **473** 3871–3888
DOI: 10.1042/BCJ20160585

criteria depending on peak purity and signal/noise (S/N) ratios and a final isomer filter. Failed spectra were automatically entered as new database entries if S/N ratio was >25, purity was <1.0 and presence in the biological study design class was >80%. Quantification was reported as peak height using the unique ion as default, unless a different quantification ion was manually set in the BinBase administration software BinView. A quantification report table was produced for all database entries that were positively detected in >10% of the samples of a study design class (as defined in the miniX database) for unidentified metabolites. A subsequent postprocessing module was employed to automatically replace missing values from the *.cdf files. Replaced values were labeled as 'low confidence' by color-coding, and for each metabolite, the number of high-confidence peak detections and the ratio of the average height of replaced values to high-confidence peak detections were recorded. These ratios and numbers were used for manual curation of automatic report datasets to datasets released for submission. Metabolites were identified by matching the ion chromatographic retention index, accurate mass and mass spectral fragmentation signatures with reference library entries created from authentic standard metabolites under the identical analytical procedure as the experimental samples.

Statistics

Post hoc analysis to compute the achieved power given the actual sample size utilized in the present study ($\alpha = 0.05$) indicated that it was >0.999 when performed with these outcomes (G*Power, v.3.0.10). Metabolite identification was performed through the use of several databases, including PubChem Compound [33], KEGG [34] and HMDB [35–37], and the online chemical translation service [38]. Before analysis, raw data were filtered by the presence of metabolites in at least 80% of patients, and all data were mean-centered and standardized. Identification of the characteristic metabolites with significance between clusters was performed using the partial least squares discriminant analysis (PLS-DA) method implemented in XLSTAT (version 2016.04.32331). The importance of each metabolite in the PLS-DA was evaluated by variable importance in the projection (VIP) score. The VIP score positively reflects the metabolite's influence on the classification, and metabolites with a score of >0.8 were considered important in the present study. Additionally, plasma metabolites along with their relative concentrations were also analyzed using a metabolite set enrichment analysis (MSEA). The MSEA was performed using quantitative enrichment analysis (QEA). The relative concentrations of metabolites were analyzed using the metabolic pathway-associated metabolite set library, and the enrichment analysis was performed using the globaltest package [39]. The QEA was performed using a generalized linear model to estimate a *Q*-statistic for each metabolite set, which allows describing the correlation between compound concentration and disease. The results were summarized as the average *Q*-statistics for each metabolite in the input set.

Results

Plasma metabolomics

Metabolomics was performed on plasma samples from carriers of the premutation and age- and sex-matched controls (Table 1). The average CGG repeat at the 5′-UTR of *FMR1* of the mutant allele in heterozygous carriers was 83 ± 19 (mean ± SD), whereas that of hemizygous carriers (males only) was significantly longer (123 ± 45; $P = 0.021$). In both cases, the CGG repeats were significantly longer than those observed in controls (31 ± 6; $P = 5 \times 10^{-5}$; Table 1).

A total of 143 metabolites were identified in plasma samples from these subjects. The PLS-DA was carried out to identify the performance of multiple metabolite biomarkers associated with premutation or, in other words, the predictive value of the class membership of subjects based on their metabolomic profile (Figure 1). VIP scores from the PLS-DA of all metabolites were calculated to evaluate those that contributed the most to the segregation of the diagnostic groups (VIP ≥ 0.8; Figure 1A). Considering that variables having a VIP score of ≥1.0 are interpreted as being highly influential, values between $0.8 \leq \text{VIP score} \leq 1.0$ indicate moderately influential variables, VIP scores ≤0.8 represent less important variables [40] and the VIP cutoff value of ≥0.8 (also used in other studies such as [41]) allowed the inclusion of not only potential biomarkers but also that of other metabolites with a relatively significant contribution in discriminating the groups (control vs. premutation), as well as a significant number of metabolites needed for a global interpretation of the changes in the metabolic pathways. Using the above-mentioned cutoff, the number of metabolites discriminating the premutation carriers from controls was reduced to 64 (48% of all originally identified). Following the BRITE classification within the KEGG database, plasma metabolites with biological roles were divided into the following

Biochemical Journal (2016) **473** 3871–3888
DOI: 10.1042/BCJ20160585

A

Compound name	KEGG	PubChem	VIP	FC	Compound name	KEGG	PubChem	VIP	FC
sucrose	C00089	5988	1.216	2.3	*naproxen*	C01517	156391	0.914	-1.0
methionine	C00073	6137	1.809	1.5	oxalic acid	C00209	971	1.133	-1.0
lactic acid	C00186	3486	0.960	1.5	succinic acid	C00042	1110	0.860	-1.0
galacturonic acid	C00333	3627	1.571	1.4	15-methylhexadecanoic acid		164860	0.820	-1.1
aconitic acid	C00417	643757	1.686	1.4	pyroglutamic acid	C01879	7405	1.062	-1.1
UDP-glucuronic acid	C00167	17473	1.304	1.3	*benzoic acid*	C00180	243	1.638	-1.1
threitol	C16884	169019	1.488	1.3	methylmaleic acid	C02226	643798	0.821	-1.1
gulonic acid	C00800	4058	1.597	1.3	oleic acid	C00712	445639	0.870	-1.1
citrulline	C00327	9750	1.990	1.2	isoleucine	C00407	6306	0.803	-1.1
mannitol	C00392	6251	1.050	1.2	fructose	C02336	439709	0.891	-1.1
xylose	C00181	135191	1.440	1.2	2,4-dihydroxybutanoic acid		192742	1.141	-1.1
sorbitol	C00794	5780	0.967	1.2	pelargonic acid	C01601	8158	1.576	-1.1
trehalose	C01083	7427	1.352	1.2	lysine	C00047	5962	0.867	-1.1
1,2-cyclohexanedione	C06105	8369	1.478	1.2	3,6-anhydro-D-galactose	C06474	16069996	1.089	-1.1
glycine	C00037	750	1.632	1.2	ribose	C00121	5779	0.846	-1.1
glycerol	C00116	753	1.424	1.2	2-hydroxybutanoic acid	C05984	8262	1.230	-1.1
maltose	C00208	3508	1.272	1.2	N-methylalanine		5288725	0.820	-1.2
citric acid	C00158	311	1.788	1.2	indole-3-lactate	C02043	92904	0.929	-1.2
pipecolinic acid	C00408	849	1.034	1.2	hypoxanthine	C00262	790	0.894	-1.2
glyceric acid	C00258	439194	1.452	1.2	tryptophan	C00078	6305	1.607	-1.2
1-monopalmitin	C01885	14900	0.856	1.2	histidine	C00135	6274	0.918	-1.2
proline	C00148	145742	1.315	1.2	mannose	C00159	18950	1.734	-1.2
threonic acid	C01620	4772	1.345	1.2	glycerol-alpha-phosphate	C00093	439162	1.459	-1.3
isocitric acid	C00451	5318532	1.665	1.2	3-hydroxybutyric acid	C01089	92135	1.046	-1.3
aminomalonate	C00872	100714	1.102	1.1	palmitoleic acid	C08362	445638	0.903	-1.3
adipic acid	C06104	196	1.130	1.1	cystine	C00491	595	0.845	-1.3
asparagine	C00152	6267	1.144	1.1	arachidonic acid	C00219	444899	1.012	-1.3
creatinine	C00791	588	1.441	1.1	beta-alanine	C00099	239	1.505	-1.4
allantoic acid	C00499	203	0.925	1.1	myristic acid	C06424	11005	0.830	-1.4
2,3,4-trihydroxybutanoic acid	C01620	27881043	1.454	1.1	phenylethylamine	C05332	1001	2.620	-1.6
salicylic acid	C00805	338	0.801	1.1	uric acid	C00366	1175	1.513	-2.1
1-methylgalactose	C03619	94214	0.969	1.1	oleamide	C19670	5283387	2.370	-3.5
malic acid	C00711	525	1.407	1.1					
fumaric acid	C00122	444972	1.386	1.1					
ornithine	C00077	6262	1.062	1.1					
glycerol-3-galactoside	C05401	16048618	0.896	1.1					
4-hydroxybutyric acid	C00989	10413	0.945	1.0					
tyrosine	C00082	6057	1.016	1.0					
phenylalanine	C00079	6140	0.870	1.0					
linoleic acid	C01595	5280450	0.959	1.0					
tartaric acid	C00898	444305	0.950	1.0					
gluconic acid	C00257	10690	0.887	1.0					

B

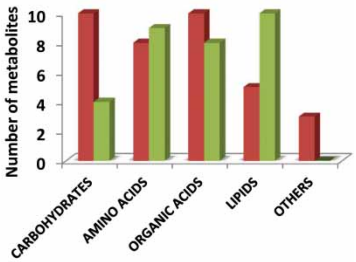

Figure 1. Plasma metabolite levels in carriers of the premutation and matched controls.

(**A**) PLS-DA of the metabolites obtained with both diagnostic groups shown with VIP ≥ 0.8 and their corresponding fold change. In italics, xenobiotics. (**B**) The number of plasma metabolites from carriers separated by their biological roles according to BRITE (KEGG database). Metabolites with biological roles were divided into the following categories: carbohydrates and related ($n = 17$); amino acids, derivatives and biogenic amines ($n = 17$); carboxylic acids ($n = 18$); lipids ($n = 15$) and others ($n = 3$). Red and green columns represent, respectively, the number of metabolites with higher and lower abundance in carriers than controls. A large format version of this figure is available as supplementary material.

categories (Figure 1B): carbohydrates and related ($n = 17$); amino acids, derivatives and biogenic amines ($n = 17$); carboxylic acids ($n = 18$); lipids ($n = 15$) and others ($n = 3$). Of note, a significant increase in metabolites belonging to the 'carbohydrate' category was observed in the premutation group, which mirrored the decline in those within the 'lipid category' (Figure 1B).

Pathway discovery analyses

By performing PLS-DA or fold-change analysis, the potential to identify subtle but consistent changes among a group of related compounds could be undermined. To overcome this obstacle, plasma metabolites along with their relative concentrations were analyzed using an MSEA. This approach identifies biologically meaningful patterns that are significantly enriched in quantitative metabolomic data. MSEA is a metabolomic version of the popular GSEA (gene set enrichment analysis) approach with its own collection of metabolite libraries analyzing directly a set of functionally related metabolites without the need to preselect compounds based on some arbitrary cutoff threshold. Metabolomic data from controls and carriers showed that the pathways significantly enriched were (in a decreasing order of significance and with false discovery rate < 0.05; Figure 2A) as follows: (i) citric acid cycle, (ii) the metabolism of the following compounds: purine, aspartate, arachidonic acid, propanoate, glycerolipid, pyruvate, β-alanine and phospholipid biosynthesis, (iii) the glycerolphosphate shuttle (which serves to transport reducing equivalents from the cytosol to mitochondria) and (iv) the metabolism of phenylacetate and betaine.

In parallel, we utilized the Pathway Analysis module of MetaboAnalyst, which combines results from the pathway enrichment analysis with the pathway topology analysis to identify the most relevant pathways in the premutation category. Pathway enrichment analysis usually refers to quantitative enrichment analysis, directly

Biochemical Journal (2016) **473** 3871–3888
DOI: 10.1042/BCJ20160585

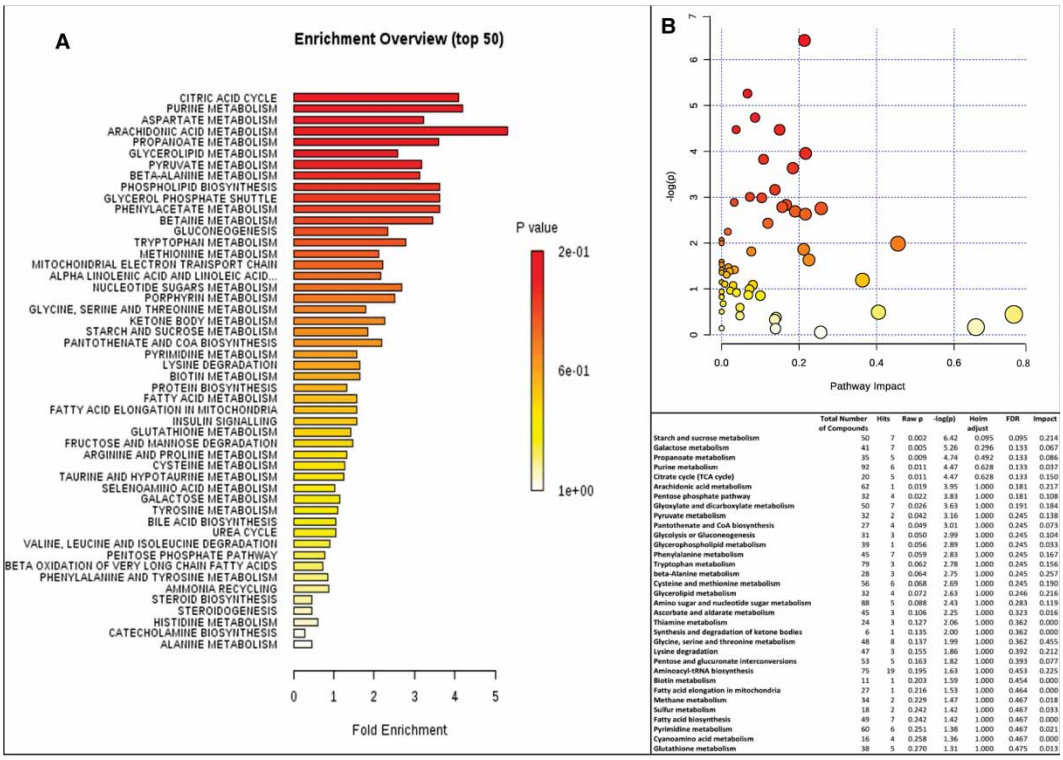

	Total Number of Compounds	Hits	Raw p	-log(p)	Holm adjust	FDR	Impact
Starch and sucrose metabolism	50	7	0.002	6.42	0.095	0.095	0.214
Galactose metabolism	41	7	0.005	5.26	0.296	0.133	0.067
Propanoate metabolism	35	5	0.009	4.74	0.492	0.133	0.086
Purine metabolism	92	6	0.011	4.47	0.628	0.133	0.037
Citrate cycle (TCA cycle)	20	5	0.011	4.47	0.628	0.133	0.150
Arachidonic acid metabolism	62	1	0.019	3.95	1.000	0.181	0.217
Pentose phosphate pathway	32	4	0.022	3.83	1.000	0.181	0.108
Glyoxylate and dicarboxylate metabolism	50	7	0.026	3.63	1.000	0.191	0.184
Pyruvate metabolism	32	2	0.042	3.16	1.000	0.245	0.138
Pantothenate and CoA biosynthesis	27	4	0.049	3.01	1.000	0.245	0.073
Glycolysis or Gluconeogenesis	31	3	0.050	2.99	1.000	0.245	0.104
Glycerophospholipid metabolism	39	1	0.056	2.89	1.000	0.245	0.033
Phenylalanine metabolism	45	7	0.059	2.83	1.000	0.245	0.167
Tryptophan metabolism	79	3	0.062	2.78	1.000	0.245	0.156
beta-Alanine metabolism	28	3	0.064	2.75	1.000	0.245	0.257
Cysteine and methionine metabolism	56	6	0.068	2.69	1.000	0.245	0.190
Glycerolipid metabolism	32	4	0.072	2.63	1.000	0.246	0.216
Amino sugar and nucleotide sugar metabolism	88	5	0.088	2.43	1.000	0.283	0.119
Ascorbate and aldarate metabolism	45	3	0.106	2.25	1.000	0.323	0.016
Thiamine metabolism	24	3	0.127	2.06	1.000	0.362	0.000
Synthesis and degradation of ketone bodies	6	1	0.135	2.00	1.000	0.362	0.000
Glycine, serine and threonine metabolism	48	8	0.137	1.99	1.000	0.362	0.455
Lysine degradation	47	3	0.155	1.86	1.000	0.392	0.212
Pentose and glucuronate interconversions	53	5	0.163	1.82	1.000	0.393	0.077
Aminoacyl-tRNA biosynthesis	75	19	0.195	1.63	1.000	0.453	0.225
Biotin metabolism	11	1	0.203	1.59	1.000	0.454	0.000
Fatty acid elongation in mitochondria	27	1	0.216	1.53	1.000	0.464	0.000
Methane metabolism	34	2	0.229	1.47	1.000	0.467	0.018
Sulfur metabolism	18	2	0.242	1.42	1.000	0.467	0.033
Fatty acid biosynthesis	49	7	0.242	1.42	1.000	0.467	0.000
Pyrimidine metabolism	60	6	0.251	1.38	1.000	0.467	0.021
Cyanoamino acid metabolism	16	4	0.258	1.36	1.000	0.467	0.000
Glutathione metabolism	38	5	0.270	1.31	1.000	0.475	0.013

Figure 2. Pathway overrepresentation analysis derived from plasma metabolomics.

(**A**) Pathways overrepresented in premutation vs. controls were obtained by utilizing the MSEA. (**B**) Metabolites were analyzed using the Pathway Analysis module of MetaboAnalyst, which combines results from the pathway enrichment analysis with the pathway topology analysis to identify the most relevant pathways in the premutation. The table includes the data with $P \leq 0.27$ associated with the pathway impact plot. A large format version of this figure is available as supplementary material.

using the compound concentration values, when compared with compound lists used by overrepresentation analysis. As indicated above, this analysis is more sensitive and has the potential to identify subtle but consistent changes among compounds involved in the same biological pathway. For this analysis, concentrations of each metabolite — normalized to averaged control values — were used as input values, Globaltest was the pathway enrichment analysis method and the node importance measure for topological analysis was the relative betweenness centrality (which measures the number of shortest paths going through the node for metabolite importance measure focusing on global network topology [42]). A graphical and detailed list of the pathways identified and their relative impact are shown in Figure 2B. The most significant ones (in a decreasing order) were carbohydrate and lipid metabolism, including galactose, propanoate, tricarboxylic acid (TCA), arachidonic acid, pentose phosphate pathway, pyruvate metabolism, pantotenate and glycolysis or gluconeogenesis.

Taken together, both analyses concurred on most of the pathways (TCA and fatty acid metabolism including glycerol phosphate shuttle) and extended some of the conclusions to other pathways (pentose phosphate pathway and gluconeogenesis).

Fatty acid and carbohydrate metabolism

Lower levels of plasma fatty acids (C9–C20) and derivatives were observed in carriers vs. controls (Figure 1A and Table 2). These findings along with elevated levels of adipic acid (a dicarboxylic acid), glycine and glycerol and lower levels of the ketone body 3-hydroxybutyrate resembled some of the features — although not as marked — of the nonketotic, hyperglycinemia with glyceric acidemia syndrome. This scenario may be interpreted as an increased lipolysis (higher glycerol), followed by increased hepatic fatty acid oxidation [decreased circulating free fatty acids (FFAs), preferentially outside mitochondrial fatty acid oxidation] to fuel the hepatic gluconeogenesis pathway. The fact that glycine levels were higher in carriers than those in controls is suggestive of a decreased

Biochemical Journal (2016) **473** 3871–3888
DOI: 10.1042/BCJ20160585

Table 2. Fatty acid levels and ratios in plasma of carriers and controls

Outcome	log 2 P/C ratio	*P*-value
Saturated fatty acids		
Pelargonic acid	−1.12	0.015
Lauric acid	−1.12	0.218
Myristic acid	−1.38	0.079
Palmitic acid	−1.06	0.332
Stearic acid	−1.02	0.395
Behenic acid	−1.10	0.225
Arachidic acid	−1.01	0.399
Monounsaturated fatty acids		
Palmitoleic acid	−1.64	0.018
Oleic acid	−1.36	0.025
Polyunsaturated fatty acids		
n-3 PUFA		
Docosahexaenoic acid	1.09	0.179
n-6 PUFA		
Linoleic acid	1.02	0.232
Arachidonic acid	−1.27	0.021
Ratio of *n*-3/*n*-6	−1.38	0.015
Estimation of enzymatic activity		
SCD index (Δ6D and Δ5D; 20:4 *n*-6/20:3 *n*-6)	−1.30	0.039
SCD *n*-7 index (SCD-16; 16:1 *n*-7/16:0)	−1.46	0.017
SCD *n*-9 index (SCD-18; 18:1 *n*-9/18:0)	−1.21	0.075
SCD index (MUFA/SFA)	−1.38	0.015
De novo lipogenesis index (16:0/18:2 *n*-6)	−1.12	0.106
Elongation index (18:0/16:0)	1.05	0.079

activity of the mitochondrial glycine cleavage system. If this were the case, an imbalanced redox status could be occurring in mitochondria characterized by higher [NADH]/[NAD^+] ratios. Higher [NADH]/[NAD^+] ratios may inhibit NAD-dependent dehydrogenases, such as pyruvate dehydrogenase complex (PDHC), α-ketoglutarate dehydrogenase and isocitrate dehydrogenase. The lower entry of pyruvate into the TCA via PDHC could result in two options: (1) to form oxaloacetate via the anaplerotic reaction catalyzed by pyruvate carboxylase or (2) to form lactate via lactate dehydrogenase (Figure 3).

In support of the latter option, several intermediates of the TCA cycle, especially those located within the first half of the cycle — namely citrate, aconitate, isocitrate, some TCA analogs (such as tartaric acid and 3-hydroxymalic acid), and lactate were higher in carriers than in controls (1.6- to 1.9-fold) suggesting a lower TCA activity (Figure 3). Furthermore, the higher ratio of Gln-to-Glu observed in plasma of premutations compared with controls (2.3-fold) suggested an increased flux from TCA to Gln, while the higher 4-hydroxybutyrate levels (GHB, a GABA derivative) suggested an increased synthesis of GABA from Glu. Of note, the higher ratio of GHB-to-succinate in carriers than in controls (2.2-fold; $P = 0.035$) is indicative of a lower succinic semialdehyde dehydrogenase (SSADH) activity, probably due to either a direct oxidation of critical Cys [43] (e.g. increased oxidative stress conditions within mitochondria) or genetics contributing to the premutation phenotype.

Fatty acids in prostaglandin pathways

To gain a deeper understanding of the fatty acid profile in carriers, we evaluated both the levels of free fatty acids between controls and carriers of the premutation and their ratios, which are predictive of the activation of prostaglandins of the series 2 vs. series 3.

Biochemical Journal (2016) **473** 3871–3888
DOI: 10.1042/BCJ20160585

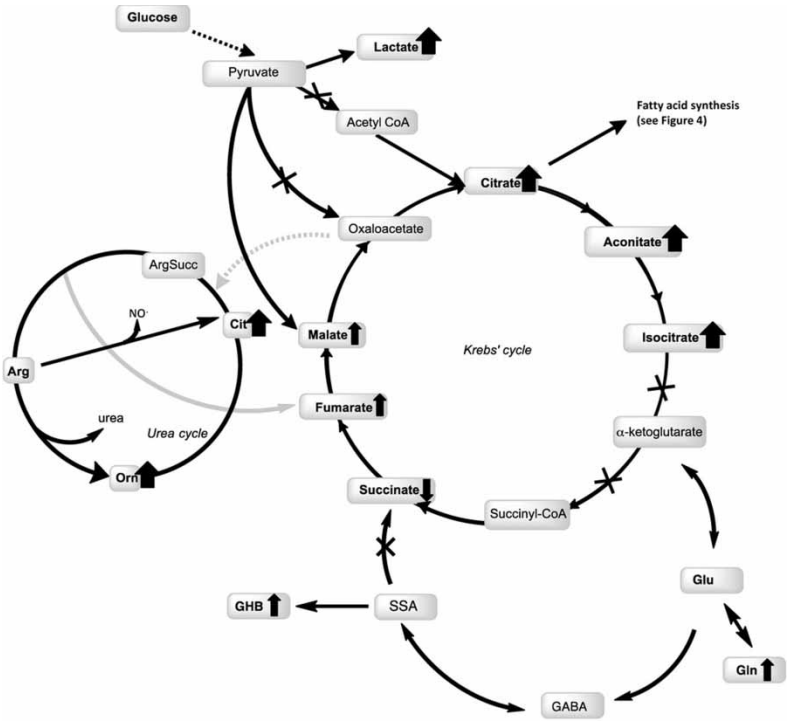

Figure 3. Overview of metabolites related to glycolysis and bioenergetics in the premutation.
Metabolites identified in the present study are shown in bold. Bold wide arrows depict strong alterations (log 2 ≥±1.2; increase if up or decrease if down), whereas thinner ones indicate moderate fold changes (log 2 ≥±1.1). Gln in the production of GABA and α-ketoglutarate in the Krebs' cycle is also shown. The lower entry of pyruvate into the TCA via PDHC could result in two options: 1) to form oxaloacetate via the anaplerotic reaction catalyzed by pyruvate carboxylase or 2) form lactate via lactate dehydrogenase. In support of the latter, several intermediates of the TCA cycle (citrate, aconitate and isocitrate), some TCA analogs (tartaric acid or 3-hydroxymalic acid) and lactate were found significantly higher in carriers, suggesting a lower TCA activity. Furthermore, the higher ratio of Gln-to-Glu observed in plasma of premutations compared with that of controls suggested an increased flux from TCA to Gln, whereas the higher levels of GHB suggested an increased synthesis of GABA from Glu. The higher observed ratio of GHB-to-succinate in carriers is indicative of a lower SSADH activity, probably due to either a direct oxidation of critical Cys (e.g. increased oxidative stress conditions within mitochondria) or genetics contributing to the premutation phenotype. Other abbreviations used: GABA, 4-aminobutyric acid; GHB: 4-hydroxybutyrate; SSA, succinic semialdehyde; Cit, citrulline.

The levels of pelargonic, palmitoleic, oleic and arachidonic acids were lower than those of controls (respectively, −1.12, −1.64, −1.36, −1.47 with $P = 0.015$, 0.018, 0.025, 0.021; Figure 1A and Table 2) as well as the ratio of fatty acids of the *n*-3 series over the *n*-6 series (docosahexaenoic acid over that of linoleic and arachidonic acids; −1.38-fold; $P = 0.015$; Table 2). The levels of myristic acid followed the same trend as those of other fatty acids (−1.38 of controls) but without reaching a statistical significance ($P = 0.079$). Fatty acid ratios were used to estimate enzymatic activities of steps involved in fatty acid desaturation, elongation and *de novo* lipogenesis (Figure 4 and Table 2). As such, the estimation of the activity of the stearoyl-CoA desaturase (SCD-1), the rate-limiting enzyme in monounsaturated fatty acid biosynthesis, which converts palmitic to palmitoleic and stearic acid to oleic acid, was calculated as the SCD-16 (C16:1 *n*-7/C16:0) and SCD-18 (C18:1 *n*-9/C18:0) ratios as described previously [44]. The SCD-16 (C16:1 *n*-7/C16:0) was significantly lower in carriers than in controls (−1.46; $P = 0.017$; Table 2), indicating that the synthesis of palmitoleic acid was lower in these subjects. Similarly, the SCD-18 (C18:1 *n*-9/C18:0), which promotes the endogenous synthesis of oleic acid from stearic acid, followed a similar trend but without reaching statistical significance (−1.21; $P = 0.075$; Table 2). The monounsaturated-to-saturated fatty acid ratio [MUFA/SFA = (C18:1 *n*-9 + C16:1 *n*-7)/(C18:0 + C16:0); Table 2] also used as an index of the desaturase activity, confirmed the previous findings, and it was significantly lower in carriers than controls (−1.38; $P = 0.015$; Table 2).

Biochemical Journal (2016) **473** 3871–3888
DOI: 10.1042/BCJ20160585

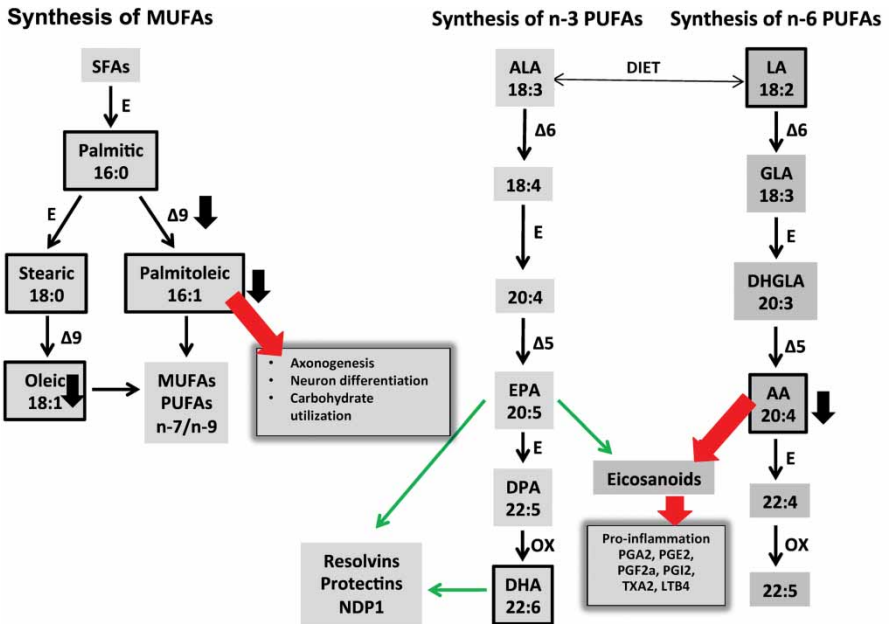

Figure 4. Overview of metabolites identified in the premutation in the context of the biosynthesis of fatty acids and eicosanoids.
Different fatty acid ratios were used to estimate enzymatic activities of steps involved in fatty acid desaturation, elongation and *de novo* lipogenesis. The ratio of arachidonic to linoleic acid (C20:4 *n*-6/C18:2 *n*-6) was evaluated as an index of the activation of the pathway, leading to the formation of prostaglandins of the 2 series starting from linoleic acid, via the formation of arachidonic acid. An increased pro-inflammatory status in carriers was inferred from the lower ratio of fatty acids of the *n*-3 series over that of the *n*-6 series, as prostaglandins generated via the Δ5–6 desaturase pathway are more pro-inflammatory than those originated from α-linolenic acid which generates prostaglandins of the 3 series (thick red arrows vs. thin green arrows). Boxed metabolites were identified by metabolomics. Black, thick arrows are based on the abundance indicated under Table 2.
Abbreviations: ALA, α-linolenic acid; LA, linoleic acid; EPA, eicosapentaenoic acid; DPA, docosapentaenoic acid; DHA, docosahexaenoic acid; AA, arachidonic acid; DHGLA, dihomo-γ-linolenic acid; MUFAs, monounsaturated fatty acids; PUFAs, polyunsaturated fatty acids; SFAs, saturated fatty acids; E, elongase; desaturases are indicated as Δ followed by the bond affected; OX, peroxisomal β-oxidation. Eicosanoids with anti-inflammatory properties (resolvins and protectins) are indicated with thin green arrows, whereas pro-inflammatory (prostanglandins of the series 2 and LTB4) are indicated with thick red arrows.

The ratio of arachidonic to linoleic acid (C20:4 *n*-6/C18:2 *n*-6) was evaluated as an index of the activation of the pathway, leading to the formation of prostaglandins of the 2 series (PGA2, PGE2, PGF2α, PGI2, TXA2 and LTB4; Figure 4) starting from linoleic acid, via the formation of arachidonic acid. This ratio (Δ6D and Δ5D in Table 2) was significantly lower in carriers than in controls (−1.30; $P = 0.039$; Table 2), suggesting a lower activation of the *n*-6 long-chain polyunsaturated fatty acids (i.e. Δ6D and Δ5D) or, more likely, an increased generation of prostaglandins of the series 2 from arachidonic acid which is not met by the demand.

Increased oxidative stress

Increased mitochondrial ROS production, elevated biomarkers of lipid and protein oxidative–nitrative damage and decreased antioxidant defenses have been observed in lymphocytes, postmortem brain samples and fibroblasts from premutation individuals [11,45,46]. Consistent with these findings, increased levels of metabolites derived from oxidative stress-mediated damage to proteins (aminomalonate) and carbohydrates (galacturonic acid) were also noted in the plasma of carriers. Lower levels of the amino acid derivative β-Ala can result from lower catabolism of carnosine (dipeptide of β-Ala and His taken from diet or synthesized in muscle or brain by carnosine synthetases), anserine (dipeptide of β-Ala and MethylHis), dihydrouracil or coenzyme A. Carnosine has been claimed to serve as a quencher of lipid peroxidation products, such as 4-hydroxy-2-nonenal and malondialdehyde, to preclude glycation of proteins [47,48] and to prevent neuronal cell death [49,50]. The fact that lower levels of both β-Ala (−1.4-fold) and His (−1.2-fold) were observed in plasma from carriers compared

Biochemical Journal (2016) 473 3871–3888
DOI: 10.1042/BCJ20160585

with controls (Figure 1) might suggest an increased cross-linking of carnosine with peroxidation or oxidation products in an attempt to control increases in oxidative stress.

Plasma sorbitol and threonic acid (probably derived from glycated proteins) levels were significantly increased in plasma from premutation carriers (1.2-fold for both; Figure 1). While sorbitol has been linked to intestinal dysfunction [51], increases in both sorbitol and threonic acid concentrations in carriers are more consistent with those in oxidative stress [52] as a result of a hyperactivation of the polyol metabolic pathway.

Damaged proteins are rapidly catabolized, and the excess of nitrogen is disposed of as urea. Indeed, the levels of citrulline and ornithine were higher (1.2- and 1.1-fold, respectively; Figure 1) in plasma from carriers than in controls, which may indicate an increased activity of the urea cycle.

In terms of antioxidant defenses, the higher levels of xylose (1.2-fold; Figure 1), erythritol (1.3-fold; Figure 1) and threitol (1.3-fold; Figure 1), probably to increase the availability of NADPH for antioxidant defenses, inferred higher glucose flux through the pentose phosphate pathway. However, the lower levels of both reduced and oxidized Cys (−1.3-fold; Figure 1), 3-hydroxybutyrate (−1.3-fold; Figure 1) and the higher levels of Met (1.5-fold; Figure 1) were suggestive of a shift of homocysteine toward the transmethylation pathway (increased Met) from the transsulfuration one (to form Cys, 2-hydroxybutyrate). This shift may have an impact on the antioxidant response, for Cys is a required building block for glutathione synthesis.

A lower turnover of RNA (including mRNA) and DNA is supported by the lower plasma levels of hypoxanthine (−1.2-fold; Figure 1), allantoic (oxidation product of uric acid) and uric acids (purine metabolism; 1.1- and −2.1-fold, respectively; Figure 1), β-Ala (dihydrouracil; −1.4-fold; Figure 1) and aminoisobutyric acid (pyrimidine catabolism; −1.2-fold). These lower levels may suggest a decreased repair capacity of nucleic acids [53,54], a decreased transcription rate (decreased protein synthesis) and/or a lower rate of cell division.

Correlation with CGG repeat expansion

Considering that many mitochondrial outcomes (i.e. protein expression of ATPB, MnSOD and cytochrome *c* oxidase, subunit IV), as well as oxidative stress markers (nitrated ATPB), correlated with the CGG expansion in fibroblasts from carriers aged 41–81 years [11], and that the CGG expansion has also been shown to directly correlate with a disrupted/fragmented mitochondrial network [14], we tested whether plasma metabolite levels correlated with the triplet nucleotide expansion. From 143 metabolites, only 23 correlated significantly with CGG repeats, with 15 of them showing a direct correlation (Figure 5A and Supplementary Material, 'Linear Regression'). Among the 15, 5 were amino acids or derivatives (Pro, Gly, hydroxyproline, citrulline and Glu-Val), 7 were carbohydrates and derivatives (1,5-anhydroglucitol, xylose, UDP glucuronic acid, maltose, threitol, glycerol-3-galactoside and lactic acid) and the rest were of different origin (creatinine, maleimide and aminomalonate). Those that followed a reciprocal correlation with the CGG expansion were three fatty acids and derivatives (pelargonic and myristic acids and oleamide), two amino acids and derivatives (Lys and methylalanine) and others (phenylethylamine, 2-hydroxyglutaric acid and phosphoenolpyruvate). Recently, we have shown that a panel of four core serum metabolites (namely, phenylethylamine, oleamide, aconitate and isocitrate) can be used for sensitive and specific diagnosis of the premutation [55], and one of these ratios (i.e. oleamide/isocitrate) showed significant potential as a specific biomarker for FXTAS [55]. Indeed, this ratio showed a trend decreasing as the stages of FXTAS increased in severity (Supplementary Figure S1). Although not significant due to the low number of carriers/stage, further research needs to expand the pool of FXTAS-affected carriers to confirm these findings (Table 1).

To derive a more refined understanding of those metabolites correlated with the CGG expansion, we manually extracted metabolite data from the OMIM, Rare Metabolic Disease, HMDB and Metagene databases for genetic diseases in which any of these metabolites matched the same trend of levels observed in the carriers (e.g. elevated lactic acid compared with controls). This manual curation process permitted a finer-tuned resolution of problems arising in the validation data, for example, from differences in metabolite nomenclature. The subset of genetic diseases that fulfilled at least one of these laboratory parameters was used to generate a list of potential enzyme or protein targets (Figure 5B). A quick glance at the identified diseases revealed that several of them are considered mitochondrial disorders (Leigh's, MELAS ≤ MERFF, Alpers' and Pearson), suggesting that the plasma metabolites that correlated with CGG expansion are indeed associated with mitochondrial dysfunction. The above-identified potential protein targets (Figure 5B) were used to build a protein–protein interaction network (Figure 5C), and these results were used for analyzing data in terms of their gene ontology (Figure 5D and Supplementary Material). In support of the previous conclusions, the most significant cellular component was identified as mitochondrion, followed by cytosol, and myelin sheath (Supplementary Material,

Biochemical Journal (2016) **473** 3871–3888
DOI: 10.1042/BCJ20160585

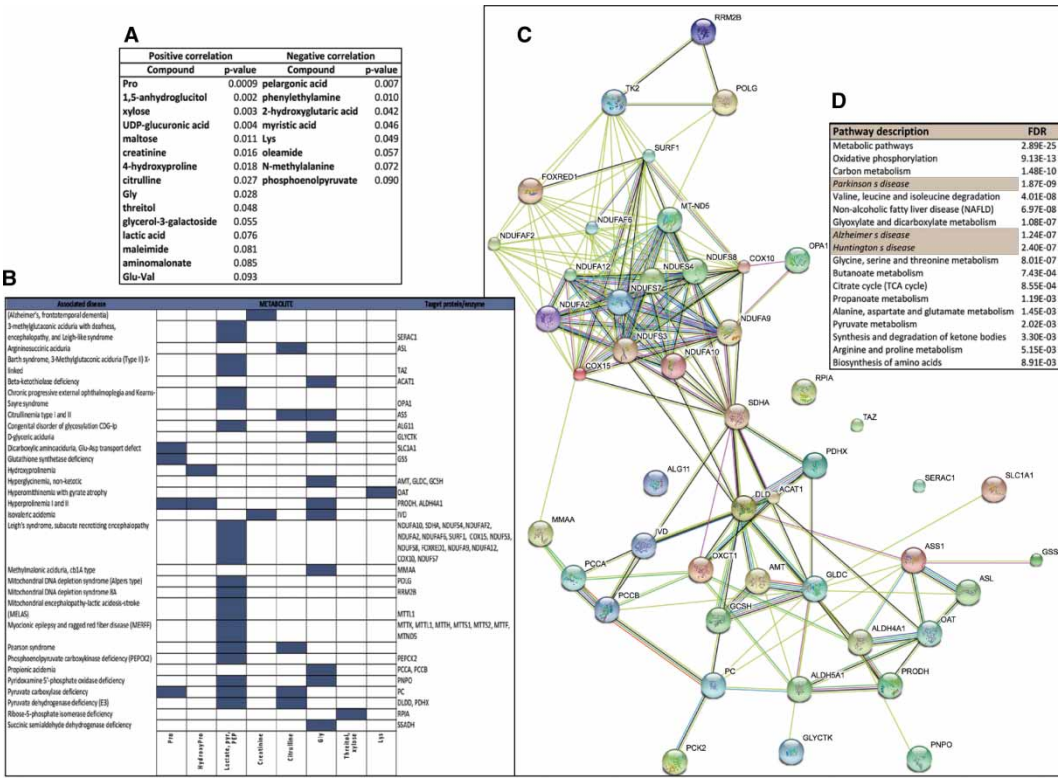

Figure 5. Correlation of plasma metabolites with CGG repeats and identification of the associated biological, cellular and molecular pathways.

(**A**) List of plasma metabolites that showed a linear correlation with CGG expansion with the corresponding *P*-values. More detailed information on the linear regression analysis is presented in Supplementary Material. (**B**) Prediction of enzyme or protein targets for those metabolites shown under **A**, whose concentrations were either elevated or reduced in plasma of genetic disorders listed under OMIM, Rare Metabolic Disease, HMDB and Metagene databases. Rows represent disorders and columns represent the metabolites. If known, the causative gene's name is indicated on the right. (**C**) Using the putative targets identified under **B** as input data, a protein–protein interaction network was built with STRING. The interactions included both direct (physical) and indirect (functional) associations; they stem from computational prediction, from knowledge transfer between organisms and from interactions aggregated from other (primary) databases. Detailed information of the analysis based on gene ontology for molecular function, biological process, cellular component and pathways is shown in Supplementary Material. (**D**) The network generated under **C** was used to generate a pathway analysis with the KEGG database. The table shows the pathway/disease name (left) and false discovery rate (right). A large format version of this figure is available as supplementary material.

'Cellular Compartment'). Along with this finding, molecular function and biological process gene ontology analyses revealed oxidoreductases and mitochondria-associated processes as the most significant ones (Supplementary Material, 'Molecular Function' and 'Biological Process'). Pathway analysis, performed using the KEGG database, indicated not only the relevance of mitochondrial processes (oxidative phosphorylation, one-carbon metabolism or folate, branched chain amino acid catabolism, Gly-Ser-Thr metabolism, Kreb's cycle, Ala-Asp-Glu metabolism and ketone body metabolism) but also the connection to other neurological diseases, such as Parkinson's, Alzheimer's and another triplet nucleotide repeat disease (Huntington's disease).

Xenobiotics of pharmaceutical or dietary origin

Current metabolomic approaches, in addition to measuring metabolites originated from endogenous cellular metabolism, also detect those derived exogenously from drugs, food and cosmetics. Presumptive diet- or treatment-related findings were also noted for carriers as well as controls. Examples include, but were not limited to, food component/plant origin and pharmaceutical-related metabolites, such as salicylate, naproxen,

Biochemical Journal (2016) **473** 3871–3888
DOI: 10.1042/BCJ20160585

benzoic acid, quinic acid, gluconic acid, 1,2-cyclohexanedione and glycolic acid. From the variety of medications that both groups were receiving (see Materials and Methods), carriers were more likely to be taking antidepressants than controls (30.4 vs. 6.25%; $P < 0.0001$); among them, the most common class was the selective serotonin reuptake inhibitors ($n = 6$, including one control). However, no difference in metabolite levels was observed in our study, consistent with the lack of differences in polyunsaturated fatty acid (PUFA) levels between medicated and unmedicated subjects reported by others [56,57]. No unmedicated subjects were present in any group, but we did not find that the metabolomic data correlated with the presence of the iatrogenic compounds indicated above or with antidepressants, antipsychotics or mood stabilizers.

Discussion

The significant similarity of affected pathways, based on changes in plasma and CSF metabolites and canonical pathways observed for Alzheimer's and Parkinson's diseases [58], supports the notion that plasma could be used to depict closely biochemical fingerprints of brain changes in carriers of the premutation. In the present study, by a nontargeted plasma metabolomic screening approach in a clinically well-characterized cohort of subjects, several pathways were identified as being altered in carriers of the premutation. Although it could be argued that plasma levels of metabolites do not represent those in the brain, unesterified fatty acids readily cross the blood–brain barrier into the brain [59], representing the major peripheral form that mirrors PUFA metabolism in the brain. Additionally, it has been reported that decreases in RBC membrane PUFAs from subjects with schizophrenia correlate with the degree of demyelination in brain white matter [60].

Among the pathways affected inferred by the plasma metabolomic data, mitochondrial dysfunction was associated with a Warburg-like shift (confirming our previous study performed with lymphocytes from premutation individuals [46]) with increases in lactate levels, altered TCA intermediates and analogs, including Glu and GHB, and a pro-inflammatory state as supported by the lipid profile as well as the increases in oxidative stress-mediated damage to carbohydrates and proteins.

Biological implications of the affected pathways in the context of the premutation

Consistent with our previous findings obtained with human carriers and animal models of the premutation, the current study also identified multiple pathways related to energy metabolism and, more specifically, to mitochondrial function that were already significantly affected in the premutation cohort [11–14,61,62]. Furthermore, specific markers that were elevated or reduced in plasma of carriers and that correlated with CGG repeats identified not only mitochondrial pathways but also dysfunctional pathways shared by other neurological diseases, such as Parkinson's .

Evidence for mitochondrial dysfunction resulted from the higher levels of a dicarboxylic acid (adipate) and lactate (Table 3), both associated with mitochondrial respiratory chain disorders. Increases in TCA intermediates have also been observed in some mitochondrial diseases [63], generally associated with the formation of analogs of TCA intermediates (e.g. tartaric acid, methylmaleic acid or citraconic acid). These TCA analogs are known inhibitors of fumarase [64], which catalyzes the conversion of fumarate to malate. Indeed, fumarate concentrations were higher in premutation than in controls (Figure 1A), suggesting that excess of fumarate may inhibit AKG-dependent prolylhydroxylases. This process would stabilize HIF-1α under normoxic conditions, resulting in a constitutive activation of this factor and downstream genes, including glycolytic ones providing a mechanism for the metabolomic differences.

Besides putative energy deficits, which may accompany mitochondrial dysfunction, neurotransmission perturbations could also result from this scenario. Indeed, the altered plasma levels of Glu and GHB may signal an imbalance in neurotransmission, which is a hallmark of anxiety disorders [65] (Table 3). This is relevant considering that carriers affected with FXTAS have a higher incidence of anxiety/mood disorders, and daughters of men with FXTAS have a higher prevalence of neurological symptoms, including anxiety, when compared with noncarrier female controls [1,66,67].

Lower plasma levels of FFA in carriers may reflect (a) the higher incidence of depression in carriers as lower levels of FFA have been reported in postmortem brain samples from subjects affected with unipolar and bipolar depression [68] and (b) neurodegeneration as lower levels of oleic and arachidonic acids have been reported in frontal cortex from subjects with Alzheimer's disease [69] and with Parkinson's disease [70], respectively (Table 3).

The lower ratio of fatty acids of the *n*-3 series over that of the *n*-6 series is suggestive of learning and memory issues in carriers vs. controls (Table 3) as it has been shown that *n*-3 PUFAs foster neuronal activity [71] counteracting memory deficits in aged mice [72], enhance the expression of mitochondrial ATPase (whereas its deficiency led to deficient glucose transport in cortex; [73]), increase the expression of Glu transporters 1 and 2 influencing neurotransmission [74], ameliorate spatial memory in rats by increasing the expression of subtypes of endocannabinoid receptors [75], increase the expression of transcription factors involved in learning and memory [76] and improve brain function and decreased levels of tau phosphorylation in a mouse model of Alzheimer's disease with enhanced endogenous production of *n*-3 PUFA [77].

The significant decrease in plasma of palmitoleic acid in carriers of the premutation vs. controls along with the lower estimated enzymatic activity of SCD1 deserves further discussion, considering the role of these factors in axonogenesis, neuron differentiation and carbohydrate utilization (Table 3). Axonogenesis requires the *de novo* synthesis of monounsaturated fatty acids based on the evidence that brain-derived neurotrophic factor (BDNF) promotes axonogenesis during brain development [78] while selectively increasing intracellular levels of palmitoleic acid and SCD1 [79], and that SCD-1 is highly expressed in axotomized neurons of the regenerating facial and hypoglossal nucleus [80]. More recently, a role for palmitoleic acid as an insulin-sensitizing lipokine has been proposed (although still controversial), suggesting that lower levels of this fatty acid may limit carbohydrate utilization. This is an important observation taking into consideration that type II diabetes mellitus is associated with an increased risk of cognitive dysfunction and dementia in Alzheimer's disease [81].

An increased pro-inflammatory status in carriers was inferred from the lower ratio of fatty acids of the *n*-3 series over that of the *n*-6 series in which prostaglandins generated via the Δ5–6 desaturase pathway (or prostaglandins of the 2 series) are more pro-inflammatory than those originated from α-linolenic acid which generates prostaglandins of the 3 series [82] (Table 3 and Figure 4, thick red arrows vs. thin green arrows). In this regard, PGE2 in neural injury in Alzheimer's disease is well documented and includes modulation of protein–lipid interactions, transmembrane and transsynaptic signaling [83]. Moreover, PGE2 levels in CSF have been identified as one of the key pathways linked to Alzheimer's disease severity [58]: PGE2 is higher in patients with mild memory impairment, but lower in those with more advanced Alzheimer's disease [84].

While a pro-inflammatory state is usually accompanied by increases in free radicals, other pathways also related to oxidative stress were found affected in carriers, confirming findings recently obtained in fibroblasts from premutation individuals, in which increased mitochondrial ROS production was accompanied by increased mtDNA deletions and increased biomarkers of lipid and protein oxidative–nitrative damage [45], as well as in postmortem brain samples [11], in which increase in oxidative/nitrative stress damage was preceded by mitochondrial dysfunction. Two metabolites identified in plasma belonging to the polyol pathway, a minor metabolic pathway of glucose running parallel to glycolysis, suggested a hyperactivation of this pathway, which leads to the formation of reactive aldehydes and biomolecule damage as evidenced by several metabolites in

Table 3. Affected biochemical pathways in premutation and their association to clinical manifestations

Outcome measured	Phenotype or symptom
Increased adipate and lactate levels	*Mitochondrial respiratory chain disorders/deficits*
Increased TCA intermediates	*Mitochondrial respiratory chain disorders/deficits*
Decreased overall fatty acids levels	*Depression*
Decreased levels of oleic and arachidonic acids	*Parkinson's*, Alzheimer's
Decreased levels of *n*-3 and *n*-6 FA	Learning and memory function deficits
Decreased levels of *n*-3 over *n*-6 FA	Increased inflammation
Decreased levels of palmitoleic acid	Decreased axogenesis, neuronal differentiation, *carbohydrate utilization*
Increased mitochondria-derived oxidative stress	*Anxiety-related disorders*
Altered Glu, GHB	*Anxiety-related disorders*
Increased levels of sorbitol	*Mood disorders* *Mitochondrial dysfunction*

In italics are clinical outcomes reported in premutation individuals.

Biochemical Journal (2016) **473** 3871–3888
DOI: 10.1042/BCJ20160585

plasma (e.g. aminomalonate). Of interest, high levels of sorbitol have been reported in the CSF of subjects affected with mood disorder [85] and in cases with mitochondrial dysfunction [86] (Table 3).

Untargeted plasma metabolomics in the context of the premutation and other neurological disorders

We have recently shown that an untargeted serum metabolomic profiling approach, combined with sequential metabolite ratio analysis, has the potential to discriminate specific plasma biomarkers in FXTAS-free and FXTAS-affected carriers [55]. In particular, our results demonstrated that a panel of four core serum metabolites (phenylethylamine, oleamide, aconitate and isocitrate) could be used for sensitive and specific diagnosis of the premutation with and without FXTAS, and one of these ratios (oleamide/isocitrate) as a specific biomarker of FXTAS [55]. Here, we showed a statistically significant correlation between CGG expansion and 23 metabolites, some of which are associated with mitochondrial dysfunction (e.g. increased lactic acid) and two of them were among the biomarkers identified for carriers (phenylethylamine and oleamide) [55]. Taken together, these studies confirm previous evidence of mitochondrial deficits in human samples from carriers as well as in many cellular and animal models of the premutation [11–14,46].

The advantage of using untargeted metabolomics over traditional targeted assays relates to the detection of several hundred analytes, which could not be detected in clinical biochemical genetics laboratory even when using the full repertoire of tests available. Therefore, plasma metabolomic analysis may be an attractive alternative when the carrier's phenotype shows unusual presentation of symptoms and the clinician is considering ordering a combination of biochemical tests. One effective option would be to start with a metabolomic testing followed by endophenotype-specific testing for disorders that might be missed by metabolomic analysis. Through this approach, metabolomic analysis may expedite additional diagnosis while allowing for the possibility to identify sources of phenotypic heterogeneity within the broad umbrella of the *FMR1* premutation. It is worth reiterating that all specimens were collected, while the carriers — as well as controls — were on clinical management, designed to alleviate their clinical phenotype. Interestingly, the fact that most subjects were on multiple medications did not have an impact on our ability to identify significant differences between groups. This could be partially explained by the overlap of the medications or supplements (see Materials and Methods) and the fact that the medication did not significantly affect the metabolomic data or that the medication was not optimized for the intended treatment.

The strength of the study is in utilizing metabolomics to detect changes in a broad variety of metabolites that reflect the complexity of metabolic networks altered in carriers. The accuracy of our findings was enhanced by the selection of carriers that closely match the control group on demographic factors. Future studies will need to assess the progression of changes in the identified pathways to shed light on the mechanisms contributing to the morbidity or as indicators of disease progression, especially at the early preclinical stages while considering the effect of sex, X-inactivation ratio, CGG repeats as well as *FMR1* mRNA expression and age on the morbidity of the disorder [87–90].

Abbreviations

ACE, angiotensin converting enzyme; ADHD, attention deficit hyperactivty disorder; ATPB, ATPase beta subunit; CSF, cerebrospinal fluid; FFA, free fatty acids; *FMR1*, fragile X mental retardation 1 gene; FXPOI, fragile X-associated primary ovarian insufficiency; FXTAS, fragile X-associated tremor ataxia syndrome; GHB, 4-hydroxybutyrate; GSEA, gene set enrichment analysis; HIF-1α, hypoxia inducible factor 1 alpha; MnSOD, manganese superoxide dismutase; MS, mass spectrometry; MSEA, metabolite set enrichment analysis; MUFA, monounsaturated fatty acid; PDHC, pyruvate dehydrogenase complex; PBMC, peripheral blood mononuclear cells; PGE2, prostaglandin E2; PLS-DA, partial least squares discriminant analysis; PUFA, polyunsaturated fatty acids; QEA, quantitative enrichment analysis; RBC, red blood cells; ROS, reactive oxygen species; SCD, stearoyl-CoA desaturase; SFA, saturated fatty acid; SSADH, succinic semialdehyde dehydrogenase; TCA, tricarboxylic acid cycle; VIP, variable importance in projection.

Author Contribution

C.G. conceptualized and designed the study, wrote the manuscript and approved the final manuscript as submitted; E.N. separated the plasma from all blood samples, contributed to the writing of the manuscript, revised and approved the final version as submitted; F.T. provided the CGG repeat sizing, revised the manuscript

and approved the final manuscript as submitted; J.H. helped with the collection and classification of nutritional supplements and medications, revised and approved the manuscript as submitted; R.H. carried out clinical assessment of the subjects, wrote clinical findings, revised the manuscript and approved the final manuscript as submitted.

Funding
The present study was funded by National Institutes for Health [ES12691 and HD036071], Simons Foundation [#271406] and by the MIND Institute Intellectual and Developmental Disabilities Research Center [U54 HD079125].

Acknowledgements
We thank all subjects who participated in the present study.

Competing Interests
R.H. has received funding from Novartis, Roche/Genentech, Alcobra, Zynerba and Neuren for treatment trials in fragile X syndrome, autism and Down's syndrome. She has also consulted with Novartis and Roche/Genentech regarding treatment for fragile X syndrome. The other authors have no financial disclosures relevant to the present study.

References
1 Kogan, C.S., Turk, J., Hagerman, R.J. and Cornish, K.M. (2008) Impact of the Fragile X mental retardation 1 (FMR1) gene premutation on neuropsychiatric functioning in adult males without fragile X-associated Tremor/Ataxia syndrome: a controlled study. *Am. J. Med. Genet. B Neuropsychiatr. Genet.* **147B**, 859–872 doi:10.1002/ajmg.b.30685
2 Tassone, F., Greco, C.M., Hunsaker, M.R., Seritan, A.L., Berman, R.F., Gane, L.W. et al. (2012) Neuropathological, clinical and molecular pathology in female fragile X premutation carriers with and without FXTAS. *Genes Brain Behav.* **11**, 577–585 doi:10.1111/j.1601-183X.2012.00779.x
3 Battistella, G., Niederhauser, J., Fornari, E., Hippolyte, L., Gronchi Perrin, A., Lesca, G. et al. (2013) Brain structure in asymptomatic FMR1 premutation carriers at risk for fragile X-associated tremor/ataxia syndrome. *Neurobiol. Aging* **34**, 1700–1707 doi:10.1016/j.neurobiolaging.2012.12.001
4 Cronister, A., Schreiner, R., Wittenberger, M., Amiri, K., Harris, K. and Hagerman, R.J. (1991) Heterozygous fragile X female: historical, physical, cognitive, and cytogenetic features. *Am. J. Med. Genet.* **38**, 269–274 PMID:2018071
5 Hagerman, R.J., Leehey, M., Heinrichs, W., Tassone, F., Wilson, R., Hills, J. et al. (2001) Intention tremor, parkinsonism, and generalized brain atrophy in male carriers of fragile X. *Neurology* **57**, 127–130 PMID:11445641
6 Winarni, T.I., Chonchaiya, W., Sumekar, T.A., Ashwood, P., Morales, G.M., Tassone, F. et al. (2012) Immune-mediated disorders among women carriers of fragile X premutation alleles. *Am. J. Med. Genet. A* **158A**, 2473–2481 doi:10.1002/ajmg.a.35569
7 Wong, L.M., Goodrich-Hunsaker, N.J., McLennan, Y., Tassone, F., Harvey, D., Rivera, S.M. et al. (2012) Young adult male carriers of the fragile X premutation exhibit genetically modulated impairments in visuospatial tasks controlled for psychomotor speed. *J. Neurodev. Disord.* **4**, 26 doi:10.1186/1866-1955-4-26
8 Hagerman, R. and Hagerman, P. (2013) Advances in clinical and molecular understanding of the FMR1 premutation and fragile X-associated tremor/ataxia syndrome. *Lancet Neurol.* **12**, 786–798 doi:10.1016/S1474-4422(13)70125-X
9 Chonchaiya, W., Tardif, T., Mai, X., Xu, L., Li, M., Kaciroti, N. et al. (2013) Developmental trends in auditory processing can provide early predictions of language acquisition in young infants. *Dev. Sci.* **16**, 159–172 doi:10.1111/desc.12012
10 Farzin, F., Perry, H., Hessl, D., Loesch, D., Cohen, J., Bacalman, S. et al. (2006) Autism spectrum disorders and attention-deficit/hyperactivity disorder in boys with the fragile X premutation. *J. Dev. Behav. Pediatr.* **27**, S137–S144 PMID:16685180
11 Ross-Inta, C., Omanska-Klusek, A., Wong, S., Barrow, C., Garcia-Arocena, D., Iwahashi, C. et al. (2010) Evidence of mitochondrial dysfunction in fragile X-associated tremor/ataxia syndrome. *Biochem. J.* **429**, 545–552 doi:10.1042/BJ20091960
12 Napoli, E., Ross-Inta, C., Wong, S., Omanska-Klusek, A., Barrow, C., Iwahashi, C. et al. (2011) Altered zinc transport disrupts mitochondrial protein processing/import in fragile X-associated tremor/ataxia syndrome. *Hum. Mol. Genet.* **20**, 3079–3092 doi:10.1093/hmg/ddr211
13 Napoli, E., Ross-Inta, C., Song, G., Wong, S., Hagerman, R., Gane, L.W. et al. (2016) Premutation in the fragile X mental retardation 1 (FMR1) gene affects maternal Zn-milk and perinatal brain bioenergetics and scaffolding. *Front. Neurosci.* **10**, e1002481 doi:10.3389/fnins.2016.00159
14 Napoli, E., Song, G., Wong, S., Hagerman, R. and Giulivi, C. (2016) Altered bioenergetics in primary dermal fibroblasts from adult carriers of the FMR1 premutation before the onset of the neurodegenerative disease fragile X-associated tremor/ataxia syndrome. *Cerebellum* 1–13 doi:10.1007/s12311-016-0779-8
15 Seltzer, M.M., Baker, M.W., Hong, J., Maenner, M., Greenberg, J. and Mandel, D. (2012) Prevalence of CGG expansions of the FMR1 gene in a US population-based sample. *Am. J. Med. Genet. B Neuropsychiatr. Genet.* **159B**, 589–597 doi:10.1002/ajmg.b.32065
16 Werner, E., Heilier, J.-F., Ducruix, C., Ezan, E., Junot, C. and Tabet, J.-C. (2008) Mass spectrometry for the identification of the discriminating signals from metabolomics: current status and future trends. *J. Chromatogr. B Analyt. Technol. Biomed. Life Sci.* **871**, 143–163 doi:10.1016/j.jchromb.2008.07.004
17 Werner, E., Croixmarie, V., Umbdenstock, T., Ezan, E., Chaminade, P., Tabet, J.-C. et al. (2008) Mass spectrometry-based metabolomics: accelerating the characterization of discriminating signals by combining statistical correlations and ultrahigh resolution. *Anal. Chem.* **80**, 4918–4932 doi:10.1021/ac800094p

Biochemical Journal (2016) **473** 3871–3888
DOI: 10.1042/BCJ20160585

18 Goodacre, R., Vaidyanathan, S., Dunn, W.B., Harrigan, G.G. and Kell, D.B. (2004) Metabolomics by numbers: acquiring and understanding global metabolite data. *Trends Biotechnol.* **22**, 245–252 doi:10.1016/j.tibtech.2004.03.007

19 German, J.B., Hammock, B.D. and Watkins, S.M. (2005) Metabolomics: building on a century of biochemistry to guide human health. *Metabolomics* **1**, 3–9 doi:10.1007/s11306-005-1102-8

20 Wang, C., Kong, H., Guan, Y., Yang, J., Gu, J., Yang, S. et al. (2005) Plasma phospholipid metabolic profiling and biomarkers of type 2 diabetes mellitus based on high-performance liquid chromatography/electrospray mass spectrometry and multivariate statistical analysis. *Anal. Chem.* **77**, 4108–4116 doi:10.1021/ac0481001

21 Rozen, S., Cudkowicz, M.E., Bogdanov, M., Matson, W.R., Kristal, B.S., Beecher, C. et al. (2005) Metabolomic analysis and signatures in motor neuron disease. *Metabolomics* **1**, 101–108 doi:10.1007/s11306-005-4810-1

22 Scherzer, C.R., Eklund, A.C., Morse, L.J., Liao, Z., Locascio, J.J., Fefer, D. et al. (2007) Molecular markers of early Parkinson's disease based on gene expression in blood. *Proc. Natl Acad. Sci. USA* **104**, 955–960 doi:10.1073/pnas.0610204104

23 Barba, I., Fernandez-Montesinos, R., Garcia-Dorado, D. and Pozo, D. (2008) Alzheimer's disease beyond the genomic era: nuclear magnetic resonance (NMR) spectroscopy-based metabolomics. *J. Cell. Mol. Med.* **12**, 1477–1485 doi:10.1111/j.1582-4934.2008.00385.x

24 Boudonck, K.J., Mitchell, M.W., Nemet, L., Keresztes, L., Nyska, A., Shinar, D. et al. (2009) Discovery of metabolomics biomarkers for early detection of nephrotoxicity. *Toxicol. Pathol.* **37**, 280–292 doi:10.1177/0192623309332992

25 Boudonck, K.J., Rose, D.J., Karoly, E.D., Lee, D.P., Lawton, K.A. and Lapinskas, P.J. (2009) Metabolomics for early detection of drug-induced kidney injury: review of the current status. *Bioanalysis* **1**, 1645–1663 doi:10.4155/bio.09.142

26 Lawton, K.A., Berger, A., Mitchell, M., Milgram, K.E., Evans, A.M., Guo, L. et al. (2008) Analysis of the adult human plasma metabolome. *Pharmacogenomics* **9**, 383–397 doi:10.2217/14622416.9.4.383

27 Sreekumar, A., Poisson, L.M., Rajendiran, T.M., Khan, A.P., Cao, Q., Yu, J. et al. (2009) Metabolomic profiles delineate potential role for sarcosine in prostate cancer progression. *Nature* **457**, 910–914 doi:10.1038/nature07762

28 Tassone, F., Hagerman, R.J., Taylor, A.K., Gane, L.W., Godfrey, T.E. and Hagerman, P.J. (2000) Elevated levels of FMR1 mRNA in carrier males: a new mechanism of involvement in the fragile-X syndrome. *Am. J. Hum. Genet.* **66**, 6–15 doi:10.1086/302720

29 Jacquemont, S., Hagerman, R.J., Leehey, M., Grigsby, J., Zhang, L., Brunberg, J.A. et al. (2003) Fragile X premutation tremor/ataxia syndrome: molecular, clinical, and neuroimaging correlates. *Am. J. Hum. Genet.* **72**, 869–878 doi:10.1086/374321

30 Napoli, E., Tassone, F., Wong, S., Angkustsiri, K., Simon, T.J., Song, G. et al. (2015) Mitochondrial citrate transporter-dependent metabolic signature in the 22q11.2 deletion syndrome. *J. Biol. Chem.* **290**, 23240–23253 doi:10.1074/jbc.M115.672360

31 Fiehn, O., Garvey, W.T., Newman, J.W., Lok, K.H., Hoppel, C.L. and Adams, S.H. (2010) Plasma metabolomic profiles reflective of glucose homeostasis in non-diabetic and type 2 diabetic obese African-American women. *PLoS ONE* **5**, e15234 doi:10.1371/journal.pone.0015234

32 Fiehn, O., Wohlgemuth, G., Scholz, M., Kind, T., Lee do, Y., Lu, Y. et al. (2008) Quality control for plant metabolomics: reporting MSI-compliant studies. *Plant J.* **53**, 691–704 doi:10.1111/j.1365-313X.2007.03387.x

33 Kim, S., Thiessen, P.A., Bolton, E.E., Chen, J., Fu, G., Gindulyte, A. et al. (2016) Pubchem substance and compound databases. *Nucleic Acids Res.* **44**, D1202–D1213 doi:10.1093/nar/gkv951

34 Kanehisa, M., Sato, Y., Kawashima, M., Furumichi, M. and Tanabe, M. (2016) KEGG as a reference resource for gene and protein annotation. *Nucleic Acids Res.* **44**, D457–D462 doi:10.1093/nar/gkv1070

35 Wishart, D.S., Jewison, T., Guo, A.C., Wilson, M., Knox, C., Liu, Y. et al. (2013) HMDB 3.0—The human metabolome database in 2013. *Nucleic Acids Res.* **41**, D801–D807 doi:10.1093/nar/gks1065

36 Wishart, D.S., Knox, C., Guo, A.C., Eisner, R., Young, N., Gautam, B. et al. (2009) HMDB: a knowledgebase for the human metabolome. *Nucleic Acids Res.* **37**, D603–D610 doi:10.1093/nar/gkn810

37 Wishart, D.S., Tzur, D., Knox, C., Eisner, R., Guo, A.C., Young, N. et al. (2007) HMDB: the human metabolome database. *Nucleic Acids Res.* **35**, D521–D526 doi:10.1093/nar/gkl923

38 Wohlgemuth, G., Haldiya, P.K., Willighagen, E., Kind, T. and Fiehn, O. (2010) The Chemical Translation Service — a web-based tool to improve standardization of metabolomic reports. *Bioinformatics* **26**, 2647–2648 doi:10.1093/bioinformatics/btq476

39 Goeman, J.J., van de Geer, S.A., de Kort, F. and van Houwelingen, H.C. (2004) A global test for groups of genes: testing association with a clinical outcome. *Bioinformatics* **20**, 93–99 PMID:14693814

40 Eriksson, L., Byrne, T., Johansson, E., Kettaneh-Wold, N. and Wold, S. (2001) *Multi- and Megavariate Data Analysis. Principles and Applications*, Umetrics Academy, Umeå, Sweden

41 Ahmed, S.S.S.J. (2014) Systems biology in unruptured intracranial aneurysm: a metabolomics study in serum for the detection of biomarkers. *Metabolomics* **10**, 52–62 doi:10.1007/s11306-013-0551-8

42 Aittokallio, T. and Schwikowski, B. (2006) Graph-based methods for analysing networks in cell biology. *Brief. Bioinform.* **7**, 243–255 doi:10.1093/bib/bbl022

43 Kim, Y.-G., Lee, S., Kwon, O.-S., Park, S.-Y., Lee, S.-J., Park, B.-J. et al. (2009) Redox-switch modulation of human SSADH by dynamic catalytic loop. *EMBO J.* **28**, 959–968 doi:10.1038/emboj.2009.40

44 Ntambi, J.M. and Miyazaki, M. (2004) Regulation of stearoyl-CoA desaturases and role in metabolism. *Prog. Lipid Res.* **43**, 91–104 PMID:14654089

45 Song, G., Napoli, E., Wong, S., Hagerman, R., Liu, S., Tassone, F. et al. (2016) Altered redox mitochondrial biology in the neurodegenerative disorder fragile X-tremor/ataxia syndrome: use of antioxidants in precision medicine. *Mol. Med.* **22** doi:10.2119/molmed.2016.00122

46 Napoli, E., Song, G., Schneider, A., Hagerman, R., Eldeeb, M.A., Azarang, A. et al. (2016) Warburg effect linked to cognitive-executive deficits in FMR1 premutation. *FASEB J.* doi:10.1096/fj.201600315R

47 Guiotto, A., Ruzza, P., Babizhayev, M.A. and Calderan, A. (2007) Malondialdehyde scavenging and aldose-derived Schiff bases' transglycation properties of synthetic histidyl-hydrazide carnosine analogs. *Bioorg. Med. Chem.* **15**, 6158–6163 doi:10.1016/j.bmc.2007.06.029

48 Reddy, V.P., Garrett, M.R., Perry, G. and Smith, M.A. (2005) Carnosine: a versatile antioxidant and antiglycating agent. *Sci. Aging Knowledge Environ.* **2005**, pe12 doi:10.1126/sageke.2005.18.pe12

49 Baek, S.-H., Noh, A.R., Kim, K.-A., Akram, M., Shin, Y.-J., Kim, E.-S. et al. (2014) Modulation of mitochondrial function and autophagy mediates carnosine neuroprotection against ischemic brain damage. *Stroke* **45**, 2438–2443 doi:10.1161/STROKEAHA.114.005183

50 Kulebyakin, K., Karpova, L., Lakonsteva, E., Krasavin, M. and Boldyrev, A. (2012) Carnosine protects neurons against oxidative stress and modulates the time profile of MAPK cascade signaling. *Amino Acids* **43**, 91–96 doi:10.1007/s00726-011-1135-4
51 Cavanna, A., Molino, G., Ballarè, M., Torchio, M., Fracchia, M., Avagnina, P. et al. (1987) Non-invasive evaluation of portal-systemic shunting in man by D-sorbitol bioavailability. *J. Hepatol.* **5**, 154–161 PMID:3693859
52 Johansen, J.S., Harris, A.K., Rychly, D.J. and Ergul, A. (2005) Oxidative stress and the use of antioxidants in diabetes: linking basic science to clinical practice. *Cardiovasc. Diabetol.* **4**, 5 doi:10.1186/1475-2840-4-5
53 Pang, B., McFaline, J.L., Burgis, N.E., Dong, M., Taghizadeh, K., Sullivan, M.R. et al. (2012) Defects in purine nucleotide metabolism lead to substantial incorporation of xanthine and hypoxanthine into DNA and RNA. *Proc. Natl Acad. Sci. USA* **109**, 2319–2324 doi:10.1073/pnas.1118455109
54 Bass, B.L. (2002) RNA editing by adenosine deaminases that act on RNA. *Annu. Rev. Biochem.* **71**, 817–846 doi:10.1146/annurev.biochem.71.110601.135501
55 Giulivi, C., Napoli, E., Tassone, F., Halmai, J. and Hagerman, R. (2016) Plasma biomarkers for monitoring brain pathophysiology in FMR1 premutation carriers. *Front. Mol. Neurosci.* **9**, 1133 doi:10.3389/fnmol.2016.00071
56 Saunders, E.F.H., Reider, A., Singh, G., Gelenberg, A.J. and Rapoport, S.I. (2015) Low unesterified:esterified eicosapentaenoic acid (EPA) plasma concentration ratio is associated with bipolar disorder episodes, and omega-3 plasma concentrations are altered by treatment. *Bipolar Disord.* **17**, 729–742 doi:10.1111/bdi.12337
57 Chiu, C.C., Huang, S.Y., Su, K.P., Lu, M.L., Huang, M.C., Chen, C.C. et al. (2003) Polyunsaturated fatty acid deficit in patients with bipolar mania. *Eur. Neuropsychopharmacol.* **13**, 99–103 PMID:12650953
58 Trushina, E., Dutta, T., Persson, X.-M., Mielke, M.M. and Petersen, R.C. (2013) Identification of altered metabolic pathways in plasma and CSF in mild cognitive impairment and Alzheimer's disease using metabolomics. *PLoS ONE* **8**, e63644 doi:10.1371/journal.pone.0063644
59 Ouellet, M., Emond, V., Chen, C.T., Julien, C., Bourasset, F., Oddo, S. et al. (2009) Diffusion of docosahexaenoic and eicosapentaenoic acids through the blood-brain barrier: an in situ cerebral perfusion study. *Neurochem. Int.* **55**, 476–482 doi:10.1016/j.neuint.2009.04.018
60 Peters, B.D., Duran, M., Vlieger, E.J., Majoie, C.B., den Heeten, G.J., Linszen, D.H. et al. (2009) Polyunsaturated fatty acids and brain white matter anisotropy in recent-onset schizophrenia: a preliminary study. *Prostaglandins Leukot. Essent. Fatty Acids* **81**, 61–63 doi:10.1016/j.plefa.2009.04.007
61 Conca Dioguardi, C., Uslu, B., Haynes, M., Kurus, M., Gul, M., Miao, D.-Q. et al. (2016) Granulosa cell and oocyte mitochondrial abnormalities in a mouse model of fragile X primary ovarian insufficiency. *Mol. Hum. Reprod.* **22**, 384–396 doi:10.1093/molehr/gaw023
62 Kaplan, E.S., Cao, Z., Hulsizer, S., Tassone, F., Berman, R.F., Hagerman, P.J. et al. (2012) Early mitochondrial abnormalities in hippocampal neurons cultured from *Fmr1* pre-mutation mouse model. *J Neurochem.* **123**, 613–621 doi:10.1111/j.1471-4159.2012.07936.x
63 Crippa, B.L., Leon, E., Calhoun, A., Lowichik, A., Pasquali, M. and Longo, N. (2015) Biochemical abnormalities in Pearson syndrome. *Am. J. Med. Genet. A* **167**, 621–628 doi:10.1002/ajmg.a.36939
64 van Vugt-Lussenburg, B.M.A., van der Weel, L., Hagen, W.R. and Hagedoorn, P.-L. (2013) Biochemical similarities and differences between the catalytic [4Fe-4S] cluster containing fumarases FumA and FumB from *Escherichia coli*. *PLoS ONE* **8**, e55549 doi:10.1371/journal.pone.0055549
65 McNaughton, N. (1997) Cognitive dysfunction resulting from hippocampal hyperactivity — a possible cause of anxiety disorder? *Pharmacol. Biochem. Behav.* **56**, 603–611 PMID:9130284
66 Bourgeois, J.A., Cogswell, J.B., Hessl, D., Zhang, L., Ono, M.Y., Tassone, F. et al. (2007) Cognitive, anxiety and mood disorders in the fragile X-associated tremor/ataxia syndrome. *Gen. Hosp. Psychiatry.* **29**, 349–356 PMID:17591512
67 Chonchaiya, W., Nguyen, D.V., Au, J., Campos, L., Berry-Kravis, E.M., Lohse, K. et al. (2010) Clinical involvement in daughters of men with fragile X-associated tremor ataxia syndrome. *Clin. Genet.* **78**, 38–46 doi:10.1111/j.1399-0004.2010.01448.x
68 Conklin, S.M., Runyan, C.A., Leonard, S., Reddy, R.D., Muldoon, M.F. and Yao, J.K. (2010) Age-related changes of n-3 and n-6 polyunsaturated fatty acids in the anterior cingulate cortex of individuals with major depressive disorder. *Prostaglandins Leukot. Essent. Fatty Acids* **82**, 111–119 doi:10.1016/j.plefa.2009.12.002
69 Martin, V., Fabelo, N., Santpere, G., Puig, B., Marin, R., Ferrer, I. et al. (2010) Lipid alterations in lipid rafts from Alzheimer's disease human brain cortex. *J. Alzheimers Dis.* **19**, 489–502 doi:10.3233/JAD-2010-1242
70 Fabelo, N., Martin, V., Santpere, G., Marin, R., Torrent, L., Ferrer, I. et al. (2011) Severe alterations in lipid composition of frontal cortex lipid rafts from Parkinson's disease and incidental Parkinson's disease. *Mol. Med.* **17**, 1107–1118 doi:10.2119/molmed.2011.00119
71 Robson, L.G., Dyall, S., Sidloff, D. and Michael-Titus, A.T. (2010) Omega-3 polyunsaturated fatty acids increase the neurite outgrowth of rat sensory neurones throughout development and in aged animals. *Neurobiol. Aging* **31**, 678–687 doi:10.1016/j.neurobiolaging.2008.05.027
72 Labrousse, V.F., Nadjar, A., Joffre, C., Costes, L., Aubert, A., Gregoire, S. et al. (2012) Short-term long chain omega3 diet protects from neuroinflammatory processes and memory impairment in aged mice. *PLoS ONE* **7**, e36861 doi:10.1371/journal.pone.0036861
73 Harbeby, E., Jouin, M., Alessandri, J.-M., Lallemand, M.-S., Linard, A., Lavialle, M. et al. (2012) n-3 PUFA status affects expression of genes involved in neuroenergetics differently in the fronto-parietal cortex compared to the CA1 area of the hippocampus: effect of rest and neuronal activation in the rat. *Prostaglandins Leukot. Essent. Fatty Acids* **86**, 211–220 doi:10.1016/j.plefa.2012.04.008
74 Blondeau, N., Nguemeni, C., Debruyne, D.N., Piens, M., Wu, X., Pan, H. et al. (2009) Subchronic alpha-linolenic acid treatment enhances brain plasticity and exerts an antidepressant effect: a versatile potential therapy for stroke. *Neuropsychopharmacology* **34**, 2548–2559 doi:10.1038/npp.2009.84
75 Pan, J.-P., Zhang, H.-Q., Wei-Wang, H.-Q., Guo, Y.-F., Na, X., Cao, X.-H. et al. (2011) Some subtypes of endocannabinoid/endovanilloid receptors mediate docosahexaenoic acid-induced enhanced spatial memory in rats. *Brain Res.* **1412**, 18–27 doi:10.1016/j.brainres.2011.07.015
76 Dyall, S.C., Michael, G.J. and Michael-Titus, A.T. (2010) Omega-3 fatty acids reverse age-related decreases in nuclear receptors and increase neurogenesis in old rats. *J. Neurosci. Res.* **88**, 2091–2102 doi:10.1002/jnr.22390
77 Lebbadi, M., Julien, C., Phivilay, A., Tremblay, C., Emond, V., Kang, J.X. et al. (2011) Endogenous conversion of omega-6 into omega-3 fatty acids improves neuropathology in an animal model of Alzheimer's disease. *J. Alzheimers Dis.* **27**, 853–869 doi:10.3233/JAD-2011-111010
78 Cohen-Cory, S. and Fraser, S.E. (1995) Effects of brain-derived neurotrophic factor on optic axon branching and remodelling in vivo. *Nature* **378**, 192–196 doi:10.1038/378192a0
79 Suzuki, S., Hongli, Q., Okada, A., Kasama, T., Ohta, K., Warita, K. et al. (2012) BDNF-dependent accumulation of palmitoleic acid in CNS neurons. *Cell. Mol. Neurobiol.* **32**, 1367–1373 doi:10.1007/s10571-012-9863-x

Biochemical Journal (2016) **473** 3871–3888
DOI: 10.1042/BCJ20160585

80 Breuer, S., Pech, K., Buss, A., Spitzer, C., Ozols, J., Hol, E.M. et al. (2004) Regulation of stearoyl-CoA desaturase-1 after central and peripheral nerve lesions. *BMC Neurosci.* **5**, 15 doi:10.1186/1471-2202-5-15
81 Biessels, G.J., Kappelle, L.J. and Utrecht Diabetic Encephalopathy Study Group. (2005) Increased risk of Alzheimer's disease in Type II diabetes: insulin resistance of the brain or insulin-induced amyloid pathology? *Biochem. Soc. Trans.* **33**, 1041–1044 doi:10.1042/BST20051041
82 Das, U.N. (2005) A defect in the activity of Δ6 and Δ5 desaturases may be a factor predisposing to the development of insulin resistance syndrome. *Prostaglandins Leukot. Essent. Fatty Acids* **72**, 343–350 doi:10.1016/j.plefa.2005.01.002
83 Bazan, N.G., Colangelo, V. and Lukiw, W.J. (2002) Prostaglandins and other lipid mediators in Alzheimer's disease. *Prostagl. Other Lipid Mediat.* **68–69**, 197–210 PMID:12432919
84 Combrinck, M., Williams, J., De Berardinis, M.A., Warden, D., Puopolo, M., Smith, A.D. et al. (2006) Levels of CSF prostaglandin E2, cognitive decline, and survival in Alzheimer's disease. *J. Neurol. Neurosurg. Psychiatry* **77**, 85–88 doi:10.1136/jnnp.2005.063131
85 Regenold, W.T., Kling, M.A. and Hauser, P. (2000) Elevated sorbitol concentration in the cerebrospinal fluid of patients with mood disorders. *Psychoneuroendocrinology* **25**, 593–606 PMID:10840171
86 Regenold, W.T., Phatak, P., Makley, M.J., Stone, R.D. and Kling, M.A. (2008) Cerebrospinal fluid evidence of increased extra-mitochondrial glucose metabolism implicates mitochondrial dysfunction in multiple sclerosis disease progression. *J. Neurol. Sci.* **275**, 106–112 doi:10.1016/j.jns.2008.07.032
87 Alvarez-Mora, M.I., Rodriguez-Revenga, L., Feliu, A., Badenas, C., Madrigal, I. and Mila, M. (2016) Skewed X inactivation in women carrying the FMR1 premutation and its relation with fragile-X-associated tremor/ataxia syndrome. *Neurodegener. Dis.* **16**, 290–292 doi:10.1159/000441566
88 Berry-Kravis, E., Potanos, K., Weinberg, D., Zhou, L. and Goetz, C.G. (2005) Fragile X-associated tremor/ataxia syndrome in sisters related to X-inactivation. *Ann. Neurol.* **57**, 144–147 doi:10.1002/ana.20360
89 Al-Hinti, J.T., Nagan, N. and Harik, S.I. (2007) Fragile X premutation in a woman with cognitive impairment, tremor, and history of premature ovarian failure. *Alzheimer Dis. Assoc. Disord.* **21**, 262–264 doi:10.1097/WAD.0b013e31811ec130
90 Rodriguez-Revenga, L., Pagonabarraga, J., Gomez-Anson, B., Lopez-Mourelo, O., Madrigal, I., Xuncla, M. et al. (2010) Motor and mental dysfunction in mother-daughter transmitted FXTAS. *Neurology* **75**, 1370–1376 doi:10.1212/WNL.0b013e3181f73660